Time-Resolved Spectra of Sonoluminescence

Robert A. Hiller, Seth J. Putterman, and Keith R. Weninger
Physics Department, University of California, Los Angeles, California 90095
(Received 2 October 1997)

Time-correlated single-photon counting reveals that the width of flashes of sonoluminescence ranges from under 40 to over 350 ps for mixtures of various gases in water. Flash widths and emission times are independent of wavelength from the ultraviolet to the infrared. These measurements suggest that sonoluminescence originates in a plasma which quenches as its temperature drops below the ionization potential. For helium bubbles this model implies peak temperatures $\gtrsim$20 eV. [S0031-9007(97)05155-7]

PACS numbers: 78.60.Mq

The passage of sound through a fluid with a trapped bubble can yield the clocklike emission of ultraviolet flashes of light [1]. The key to attempts to understand the energy concentrating mechanism at work in sonoluminescence (SL) is the elucidation of the time scales for light emission [2,3]. Recently, Gompf *et al.* [4] demonstrated that time-correlated single-photon counting (TCSPC) [5] is capable of resolving the picosecond time scales that characterize the flash widths of SL. We have extended this very important contribution to obtain the flash widths and emission times for the entire range of wavelengths that make up the observable broadband spectrum of SL. The flash widths are found to range from 35 ps [6] for a bubble formed from a 20 torr solution of air in water to 380 ps for a 300 torr solution of 1% xenon in oxygen cooled to 4 °C. Most important is the observation that, within experimental resolution of a few ps, the flash widths and times of emission of SL are independent of wavelength. We propose that these data rule out adiabatic heating as a mechanism for SL and, furthermore, that the light is emitted during the lifetime of a high energy phase generated by extreme nonlinear processes in the bubble. In the event that the high energy phase is a plasma, the source of SL would be thermal bremsstrahlung [7].

Figure 1 shows the spectral distribution of flash width and emission times for various gas bubbles in water. The features that the flash width increases with intensity and concentration are consistent with previous measurements [4]. We also find that over the spectral range from 200 to 800 nm for SL flash width is constant to within a few picoseconds for all of the gases studied so far. Figure 1(B) shows that within a flash each wavelength is emitted at the same time. Figure 2 shows the flash width as a function of the integrated intensity of light emission for helium, xenon, and 1% xenon in oxygen solutions. For these systems the flash width is characterized by the intensity. In particular, helium and xenon bubbles have the same flash width for the same intensity.

Although TCSPC has a long established application to the measurement of fluorescence lifetimes, its application to SL [see Fig. 3] raises various artifacts and challenges. This technique is based upon the fact that photomultiplier tubes (PMTs) can localize the arrival of a photon to a time much shorter than the response time to a pulse of light. For the tubes used in these experiments (Hamamatsu R3809-U50 and R2809U) the transit time spreads can be as small as 25 ps, whereas the rise times are about 150 ps. When two tubes record the arrival times of single photons generated by a very short (200 fs) laser flash, the history of events taken through a constant fraction discriminator and time-to-amplitude converter yields the Green's function of the apparatus as displayed in Fig. 1. This response function is then compared to the data obtained when the laser is replaced with an SL bubble (also shown in Fig. 1). The flash width can be obtained by comparing the full width at half-maximum (FWHM) or, more generally, by deconvolution. In each case, we found it necessary to assume a Gaussian pulse shape.

Light from the bubble is collected to the monochromator with mirrors to eliminate chromatic aberration. An off-axis paraboloid intercepts about 2% of the SL emission, and the parallel light is focused to a real image at the input slit with an overall magnification of 3. For TCSPC the input slit was set at 1 mm, and the output slit adjusted for a reasonable count rate. For wavelengths shorter than about 650 nm the spectral resolution is 9 nm FWHM, increasing to 27 nm as the output slit was opened fully to compensate for the decreasing spectral radiance of the bubble in the red. The photon detection probability was kept low to reduce count-rate effects which decrease the observed width. Count rates less than 3% (of the 34 kHz flash repetition rate) result in less than a few percent error. Illumination of a finite number of grating rulings spreads the pulse, resulting in an additional 2 ps/100 nm convolved into the width. As the grating rotates the average path increases, resulting in a later arrival time for the red light of about 1 ps/100 nm. The data in Figs. 1 and 2 have been corrected for these effects.

Light from the bubble is also focused on a second microchannel-plate photomultiplier tube (MCP-PMT) using a quartz lens with an adjustable aperture. Chromatic aberration is less problematic with this tube [R2809U]

 0031-9007/98/80(5)/1090(4)$15.00

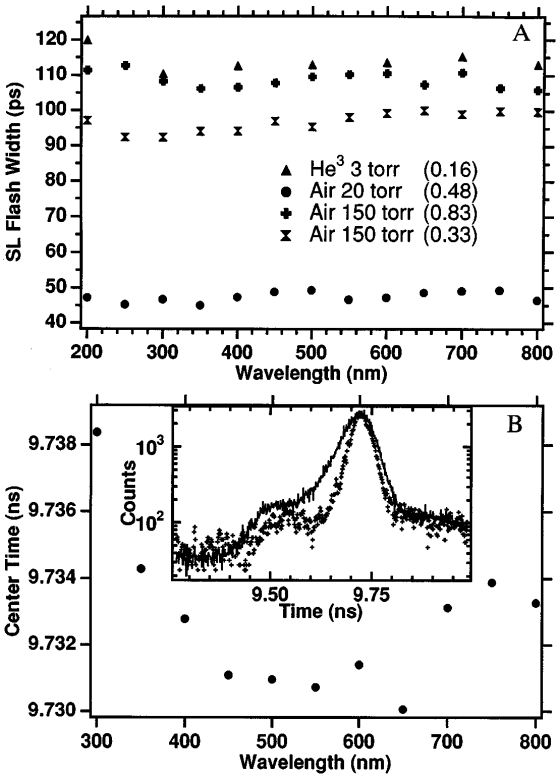

FIG. 1. Flash width (A) and relative emission time (B) of sonoluminescence as a function of wavelength, showing that these parameters are independent of the photon energy. The numbers in parentheses are intensity relative to the brightest SL from 150 torr air. (B) shows data for 20 torr air; the increase in emission time below 320 nm is due to variations in the index of refraction of water and the commercial quartz used for the acoustic resonator [the 200 nm data point lies at 9.766 ns]. The inset to (B) contains instrument and SL response functions for this system (with the light sources attenuated so that each PMT operated at the single photon level). The intrinsic jitter is represented by the full width at half-maximum of 55 ps generated by the flashes of a 200 fs laser. The outer curve (FWHM = 78 ps) is generated by an air bubble is well-degassed water (about 20 torr partial pressure).

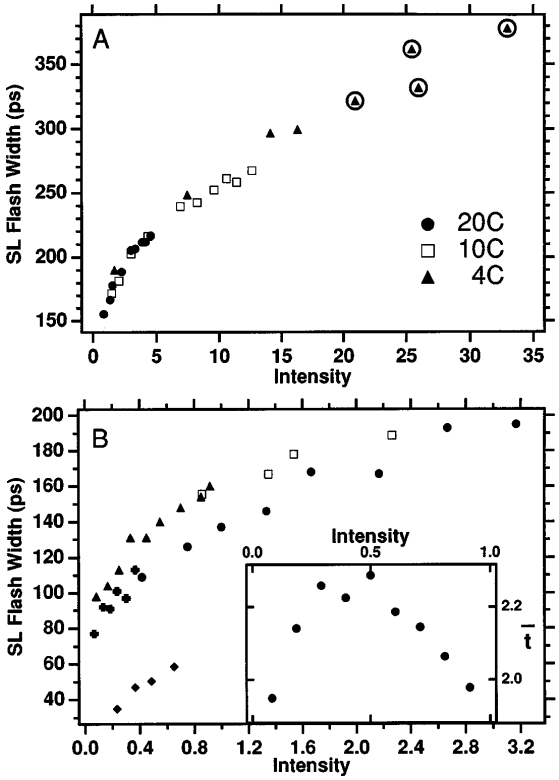

FIG. 2. Flash width at 500 nm as a function of integrated SL intensity (relative to the brightest SL from 150 torr air) for various bubbles: (A) shows data for 300 torr solution of a 1% xenon in oxygen mixture at 4, 10, 20 °C; (B) contains data for 3 torr xenon (●), 3 torr argon (▲), 3 torr helium (✚), 20 torr air (◆), and 300 torr 1% xenon in oxygen (□), all at 20 °C. Note that for the same flash intensity, 3 torr helium and 3 torr xenon have the same flash width. The circled points indicate bubbles that could be as much as 1 cm off center in the flask (as tends to happen to the brightest bubbles). The inset to (B) shows the measurements for 3 torr argon scaled to a theoretical estimate based upon the shock-wave-plasma-bremsstrahlung model of SL [7]. The drift in gas content accounts for systematic variations in flash width that are observed when a region of parameter space is remeasured on the time scale of 1 hour. This variation of about 5–10 ps is readily apparent for the six helium data points. This variation is also the accuracy with which we claim that the dimmest xenon bubble has the same flash width (at the same intensity of SL) as the brightest helium bubble. We also note that, at a given SL intensity, air and pure noble gas bubbles have significantly different flash widths.

since it has little sensitivity to wavelengths shorter than 350 nm. Data was acquired in two modes: (i) Single photon counting in each tube [5] and (ii) single photon counting at the output of the monochromator to multiple photons (about 10 photoelectrons/flash) in the second tube. (In this case, an aperture maintains a fixed light level.) To obtain measurements of the dimmest bubbles, method (i) was essential. For brighter bubbles the use of method (ii) facilitated faster data acquisition and provided a hard trigger relative to which the emission time could be measured. The emission time is the center time of the distributions such as shown in Fig. 1(B). Where both methods could be applied, the deconvolutions (which are different for these two cases) yielded consistent results.

We believe that the main sources of error in these experiments are variations in bubble intensity, and a slow drift in the bubble contents over the several hours required for a run. Use of a sealed system [3,8] limits, but does not eliminate these problems. The measured pulse width can be lengthened by imperfect alignment of the mirrors as well as by delayed light from reflections from the wall of the acoustic resonator. Chromatic dependence of the transit time spread of the PMTs is believed to be small and has not been corrected for. It is also important to note that the response function has a standard deviation which is substantially larger than the Gaussian value of FWHM/2.35.

Lack of wavelength dependence in the flash width rules out adiabatic heating as a source of SL [4,9]. This type of thermal process would yield longer flashes in the infrared,

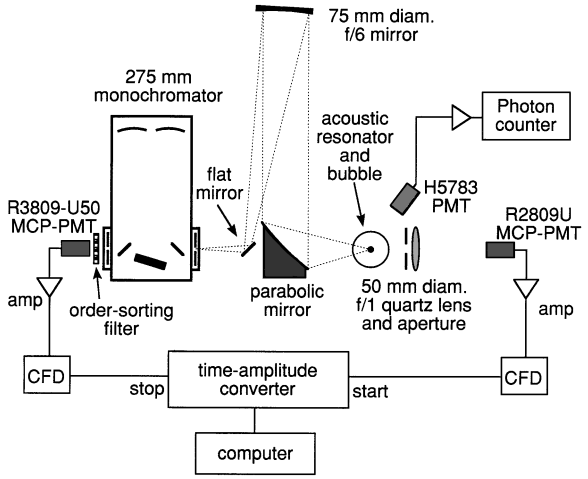

FIG. 3. Experimental arrangement used in measurements of the time-resolved spectrum of SL. The arrival time of the photons is detected with a constant fraction discriminator [EG&G 935] which triggers a time-to-amplitude converter [EG&G 566]. The computer records a histogram of measured time differences.

where the bubble would spend more time as it heats up and cools down. Based upon our observations, we propose that SL is emitted during the time that the gas is in a higher energy state such as a plasma. The light at all wavelengths turns on and off as the system enters and leaves this phase. In the proposed case where the higher energy phase is a plasma [7], the light would be emitted during the time t_{plasma} that the (electron) temperature T exceeds (or is approximately equal to) the ionization potential χ of the gas in the bubble.

In the framework of the shock wave model of SL [7,10], T jumps dramatically as the shock front reaches its smallest radius and expands back through the already heated gas. At this moment all wavelengths would turn on together. Then, as the expanding shock cools, due to its decreasing Mach number, T drops below χ/k_{B} (where k_{B} is the Boltzmann's constant), the plasma quenches, and the emission stops. This model permits a qualitative estimate of the SL time scales. Heating of the gas due to the expanding shock wave goes roughly as the fourth power of the Mach number:

$$T/T_0 \approx M^4 \approx [t_0/t]^{4(1-\alpha)},$$

where T_0 is the ambient temperature, $\alpha \sim 0.7$ is Guderley's coefficient for the imploding shock wave of radius $R_s = A|t|^{\alpha}$, and $t_0 \sim \alpha R_0/c_0$ is the characteristic time determined by an estimate of the launch condition for the imploding shock, namely, that $M = 1$ when the bubble radius R equals its ambient radius R_0 [3]. The time during which the thermal energy is larger than χ is then found to be

$$t_{\text{plasma}} \sim t_0[k_{\text{B}}T_0/\chi]^{1/4(1-\alpha)}.$$

For argon this time is about 70 ps. Shown in the inset to Fig. 2(B) is the scaled flash width ($\bar{t} = t_{\text{SL}}/t_{\text{plasma}}$, where t_{SL} is the measured width) as a function of intensity for argon dissolved into water at a partial pressure of 3 torr. This parameter is about unity, with a variation in R_0 (see Fig. 43 of Ref. [3]) accounting for the strong dependence of flash width on intensity. Whether inclusion of the van der Waals hard core [7] will lead to a simple scaling law that unifies different gases [e.g., helium and xenon] remains to be seen. In a broader sense, it must be emphasized that there is no direct experimental evidence for the existence of a shock wave or the formation of a plasma, nor has anyone succeeded in measuring the size of the light emitting region. According to the above model, one finds $R_s(t_{\text{plasma}}) \sim 0.1$ μm so that the free charge is about 10^9 electrons.

In conclusion, we note that the intensity and existence of SL are very sensitive to various experimental parameters such as the acoustic drive amplitude, ambient temperature, and the makeup of the gas-water mixture [3,8,11]. But when parameters are chosen to yield SL the resulting state has a number of "universal" characteristics. The spectra of various gas mixtures are all broadband with no lines and have the same shape. The radius versus time dynamics of SL bubbles have a similar structure, and now we have found that the emission times and flash width are independent of wavelength and that, remarkably, helium bubbles and xenon bubbles of the same intensity have the same flash width. We interpret these observations as indicating that the stressed conditions inside the collapsed bubble produce a short lived high energy phase whose qualitative properties are independent of the initial state of the bubble. SL occurs during the lifetime of this state. We propose that this state is a "cold" dense plasma. The validity of this picture could be checked via use of light scattering from the bubble's interior during

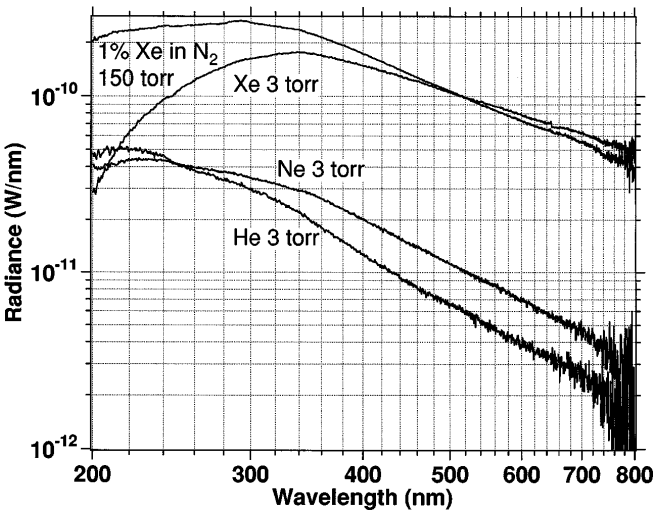

FIG. 4. High resolution (1 nm FWHM) spectra of SL from various gases in water, acquired using the optical arrangement of Fig. 3. The light is detected with a linear PMT (R2027) replacing the MCP (R3809) and the signal analyzed as in Refs. [1] and [8]. This data further restrict the presence of emission lines in single bubble sonoluminescence.

the emission time of the SL. Whether sonoluminescence is produced by shock waves could perhaps be checked by photographing the interior of the large bubbles that appear at boundaries [12]. Finally, the light collection method employed in this experiment is capable of delivering 1000 photons to a photocathode located behind a 50 μm slit without temporal dispersion or chromatic aberration. Figure 4 displays high resolution [1 nm FWHM] spectra of SL that has been obtained with this setup. In future work this arrangement will be used to acquire streak photos that might resolve the shape of an individual flash of SL.

We thank the NSF-Division of Atomic, Molecular, Optical and Plasma Physics (exp) and DOE-Division of Engineering and Geophysics (theory) for support. We acknowledge H. Fetterman, H. Erlig, and S. Wang for assistance with a ps dye laser, K. Arisaka for the loan of equipment and valuable discussions, and R. Cousins for valuable insights.

[1] R. Hiller, S. J. Putterman, and B. P. Barber, Phys. Rev. Lett. **69**, 1182 (1992).
[2] B. P. Barber and S. J. Putterman, Nature (London) **352**, 318 (1991).
[3] B. P. Barber *et al.,* Phys. Rep. **281**, 65 (1997).
[4] B. Gompf *et al.,* Phys. Rev. Lett. **79**, 1405 (1997).
[5] D. V. O'Conner and D. Phillips, *Time-correlated Single Photon Counting* (Academic Press, New York, 1984).
[6] This value is consistent with an upper bound of 50 ps [B. P. Barber *et al.,* J. Acoust. Soc. Am. **91**, 3061 (1992)] that was established for well-degassed solutions of air in water by comparing the rise times of a PMT for a flash of SL and a flash of a 34 ps laser [Hamamatsu PLP-01]. The importance of controlling and monitoring the gas concentration was appreciated at a later data [8] and so the precise gas concentrations used in the earlier experiments is not known.
[7] C. C. Wu and P. H. Roberts, Phys. Rev. Lett. **70**, 3424 (1993); C. C. Wu and P. H. Roberts, Proc. R. Soc. London A **445**, 323 (1994).
[8] R. Hiller *et al.,* Science **266**, 248 (1994).
[9] The initial stage of bubble collapse (prior to the launch of an imploding shock wave) is surely accompanied by adiabatic heating.
[10] W. C. Moss *et al.,* Phys. Fluids **6**, 2979 (1994); W. C. Moss, D. B. Clarke, and D. A. Young, Science **276**, 1398 (1997); H. P. Greenspan and A. Nadim, Phys. Fluids A **5**, 1065 (1993).
[11] B. P. Barber *et al.,* Phys. Rev. Lett. **72**, 1380 (1994).
[12] K. R. Weninger *et al.,* Phys. Rev. E **56**, 6745 (1997).